Available online at www.sciencedirect.com
ScienceDirect
Journal of Crystal Growth 300 (2007) 94–99
JOURNAL OF CRYSTAL GROWTH
www.elsevier.com/locate/jcrysgro

Nucleation conditions for catalyst-free GaN nanowires ☆

K.A. Bertness*, A. Roshko, L.M. Mansfield, T.E. Harvey, N.A. Sanford

Optoelectronics Division, National Institute of Standards and Technology, Boulder, CO, USA

Available online 8 December 2006

Abstract

We have examined the initial steps for catalyst-free growth of GaN nanowires by molecular beam epitaxy (MBE) on Si (1 1 1) substrates using AlN buffer layers. These wires form spontaneously under high N-to-Ga ratios for a growth temperature range of about 810–830 °C. Field emission scanning electron microscopy (FESEM) shows that part of the GaN forms a "matrix layer" that also grows with the [0 0 0 1] direction perpendicular to the substrate surface. This layer contains small, dense hexagonal pits in which the nanowires nucleate. Using both FESEM and atomic force microscopy (AFM), we identify the pit facets as $\{1\,0\,\bar{1}\,2\}$ planes. The nucleation studies show that the use of an AlN buffer layer is essential to the regular formation of the nanowires and matrix layers under our growth conditions. Our typical AlN buffer layer is 40–50 nm thick. We conclude that the nucleation mechanism for nanowires includes formation of nanocolumns in the AlN buffer layer. The propagation of the nanowires in GaN growth appears to be driven by differences in growth rates among crystallographic planes under N-rich conditions.

PACS: 81.07.Bc; 81.15.Hi; 81.05.Ea; 68.37.Hk; 68.35.Ct

Keywords: A1. Nanostructures; A3. Molecular beam epitaxy; B1. Nitrides; B2. Semiconducting III–V materials

1. Introduction

GaN nitride nanowires are a potential manufacturing path to low-cost, high-performance LEDs [1–3] and lasers [4,5], and are suitable for a number of electronic device applications [6]. Most semiconductor nanowires, including GaN nanowires, are grown by the vapor–liquid–solid (VLS) method, in which a metal catalyst such as gold or nickel forms the nucleation point and catalyzes further growth. Under certain growth conditions in molecular beam epitaxy (MBE), however, GaN nanowires form spontaneously, i.e., without a catalyst. In this paper, we study the morphological and crystallographic variations of this spontaneous formation process. The nanowires were found to nucleate inside hexagonal pits formed by intersecting GaN $\{\bar{1}\,1\,0\,2\}$ planes. In longer growth runs, these hexagonal pits become the matrix layer. Increasing AlN buffer layer thickness and atomic N flux (relative to Ga flux) promoted the nucleation of nanowires. Optical emission spectra for the N plasma source were analyzed to distinguish atomic N from excited molecular N_2 flux. Molecular N_2 flux was found to have a stronger influence on nanowire growth rate than on nucleation. In no case were Ga droplets observed on the nanowire or matrix surfaces. We also see evidence for thermodynamic driving forces that favor the formation of *c*-axis nanowires for this growth method. We interpret our data in terms of a growth model in which nucleation of *c*-plane nanowires usually originates at the AlN buffer surface, and the nanowire growth propagates through an enhanced sticking coefficient for the end surface relative to the sidewalls and to hexagonal pits.

2. Experiment

The specimens discussed in this paper were grown with MBE using Ga metal, Al metal, and a radio-frequency (RF) plasma-enhanced N_2 source on Si (1 1 1) substrates, unless otherwise noted. The growth sequence comprised an

☆Contribution of an agency of the U.S. government, not subject to copyright.

*Corresponding author. NIST, Mail Stop 815.04, 325 Broadway, Boulder, CO 80302, USA. Tel.: +1 303 497 5069; fax: +1 303 497 3387.
E-mail address: bertness@boulder.nist.gov (K.A. Bertness).

0022-0248/$ - see front matter © 2006 Elsevier B.V. All rights reserved.
doi:10.1016/j.jcrysgro.2006.10.209

Al pre-layer (about 0.4 nm, deposited at 700 °C), AlN buffer layer (50–100 nm, grown at 650 °C), and GaN nucleation layer (typically 150 nm) [7]. The growth conditions were intentionally chosen for a high ratio of active nitrogen species relative to Ga or Al. A typical V:III ratio based on raw beam equivalent pressure (BEP) measurements was 120 for total N species pressure to Ga beam BEP. BEP was measured with a nude ion gauge that was lowered just in front of the sample growth position before the growth run began. No correction has been made for the varying atomic sensitivity of the gauge, which is typically more sensitive to higher atomic mass elements. The variability of these measurements was about 10% relative to flux measurements made with reflection high-energy electron diffraction (RHEED) in other growth experiments. We have previously shown [7,8] that these conditions, combined with substrate temperature in the range of 810–830 °C, lead to spontaneous nucleation and growth of GaN nanowires in our growth system. Runs illustrated in this paper were performed with growth temperatures from 827 to 831 °C. The growth temperature was measured from the blackbody radiation emitted from the backside of the growth substrate and collected with a quartz light pipe running through the axis of the substrate manipulator. This emission was calibrated against a conventional optical pyrometer monitoring emission from the front side of a bare, polished silicon wafer with known emissivity. The expanded uncertainty for absolute value of the substrate temperature measurement was estimated as 8 °C.

The field emission scanning electron microscopy (FESEM) images were obtained at low electron beam energies (2.5–3.0 keV) and working distances (3–5 mm). An in-lens detector was used for the highest resolution work. Some images in Fig. 6 were obtained on a different instrument with a standard secondary electron detector and 5 keV beam voltage. Layer thicknesses were measured from FESEM cross-section images. The atomic force microscopy (AFM) images were taken in tapping mode with silicon probe tips. The optical emission from the nitrogen plasma source was collected into an optical fiber with a lens mounted on the small viewport at the outer end of the plasma tube. The collected light was dispersed with a grating monochromator and detected with a blue-enhanced silicon photodiode. The spectra were not corrected for variation in transmission efficiency or detector sensitivity. The absolute intensity of the measured spectrum was

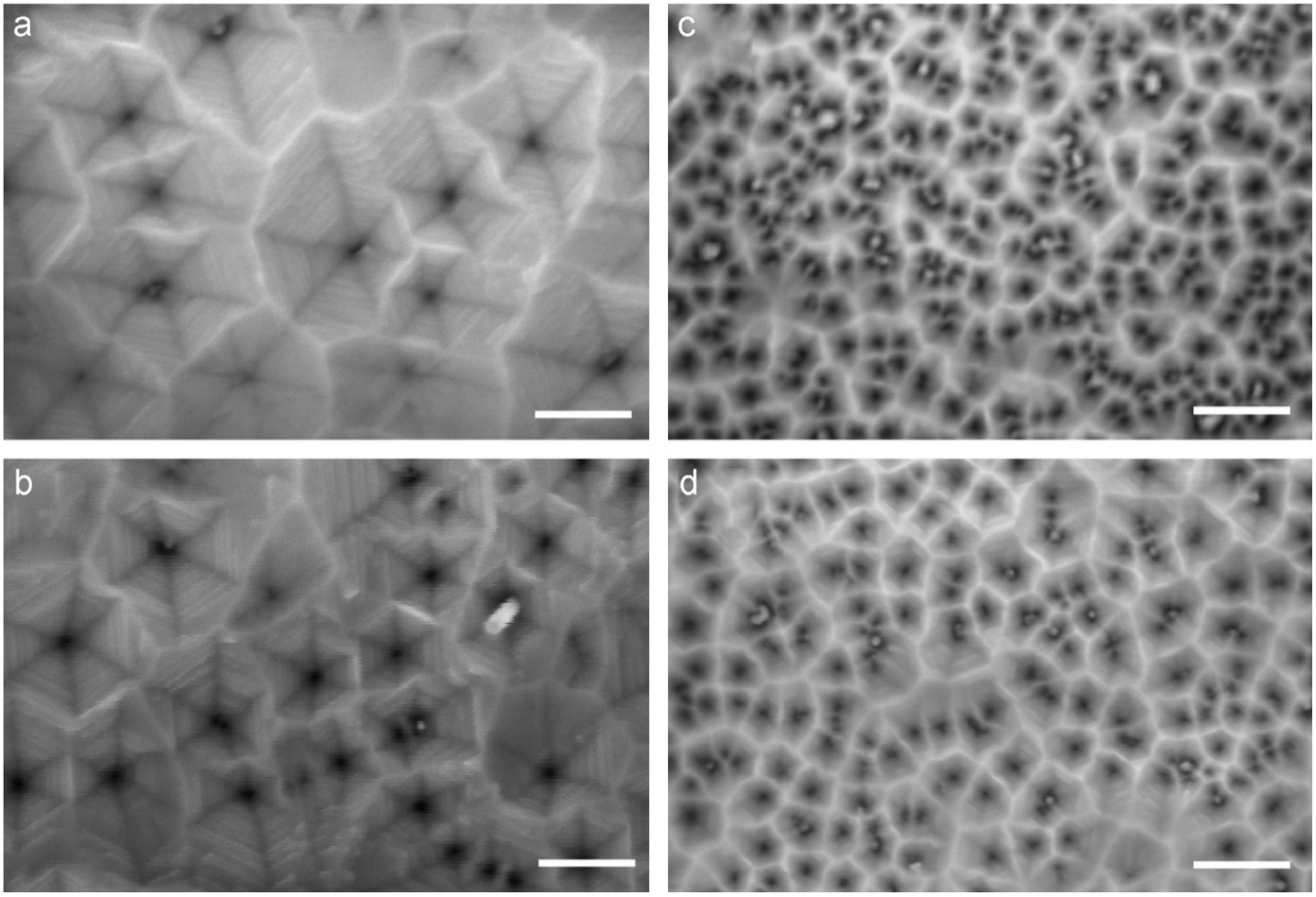

Fig. 1. Plan view FESEM images of early nucleation stages for GaN nanowires showing hexagonal faceted pits of the matrix layer and nanowires nucleated in center. Growth conditions for the pictures: (a) Ga BEP = 1.4×10^{-5} Pa, (b) Ga BEP = 1.8×10^{-5} Pa, (c) Ga BEP = 1.3×10^{-5} Pa, high atomic N in plasma and (d) Ga BEP = 0.7×10^{-5} Pa. AlN buffer layers are 50–55 nm for all four specimens. Marker bars indicate 200 nm.

unfortunately sensitive to slight changes in the mounting angle, and therefore variations in intensity from run to run were as high as 50%. Improvement of the mounting hardware is underway to eliminate this variability. The RF powers are reported as forward-going power into the plasma; reflected power was typically 1–3% of the forward power. N_2 flows were controlled and measured by a gas mass flow controller.

3. Results

Fig. 1 shows the morphologies of nucleation layers obtained with a variety of Ga BEPs and N_2 plasma conditions. For these runs, the AlN buffer layers were 50–55 nm thick, and the rough GaN matrix layers had a maximum thickness of about 150 nm. The FESEM images demonstrate that nucleation of nanowires occurred in the center of hexagonal pits with particular crystallographic orientation. Fig. 2 shows a cross-section that bisects one of the pits with the remainder of a nanowire root in the center. These features were also assessed with AFM (Fig. 3). The alignment of the features in AFM and FESEM with the substrate wafer flat indicated that the facets were tilted toward the $\langle 1\,\bar{1}\,0\,0\rangle$ directions of the crystal, and that the vertices of the pits were aligned with the Si $\langle 1\,\bar{1}\,0\rangle$ directions. As illustrated in the schematic drawing in Fig. 3, the pit facets were thus azimuthally aligned with the $\{\bar{1}\,1\,0\,0\}$ planes that form the sidewalls of a fully developed hexagonal nanowire [7]. The angle measured from the facet

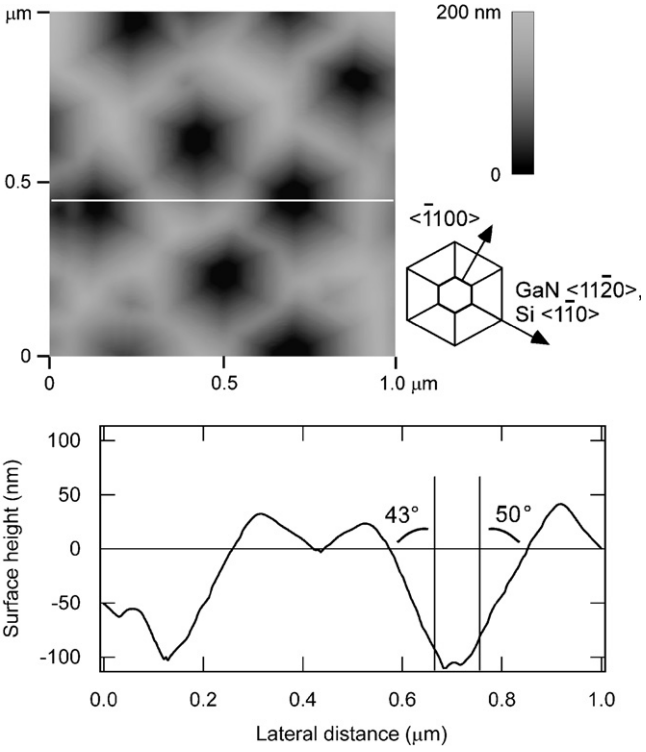

Fig. 3. AFM image and section scan for hexagonal pits for in nucleation sample from Fig. 1(a). The section scan is a slice of the three-dimensional image taken at the horizontal white line in the AFM image scan. The hexagon in the center of the schematic represents the orientation of fully developed nanowires.

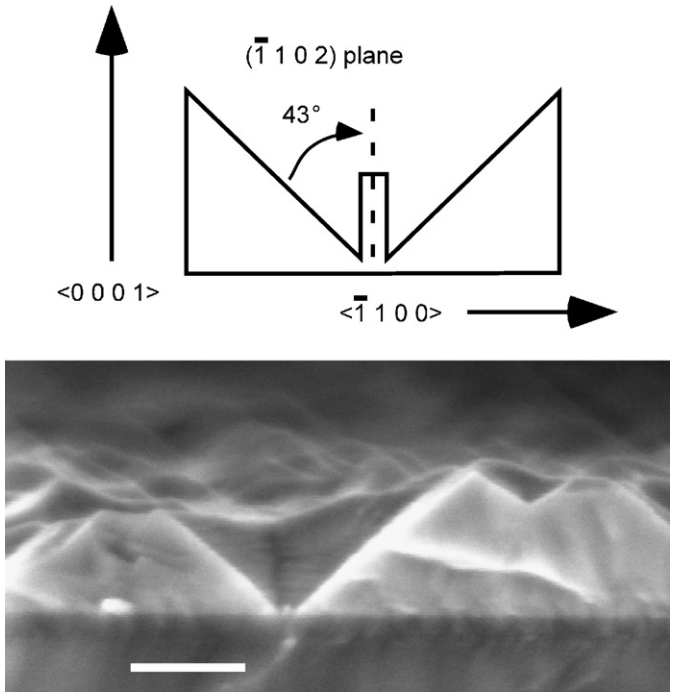

Fig. 2. Schematic illustration of nanowire nucleation within a hexagonal pit, and FESEM cross-sectional image showing one such nanowire nucleation point. Polarity of the crystal growth has not yet been determined; it is assumed to be Ga polar in the assignment of the crystal directions shown here. Marker bar indicates 200 nm.

to the specimen normal in the FESEM image is 47°, and the same average angle for the two slopes as measured with AFM is $47\pm3^\circ$. These angles are consistent with the pit sidewalls being $\{\bar{1}\,1\,0\,2\}$ planes, which make an angle of 43.2° with the (0 0 0 1) plane normal for fully relaxed lattice parameters of GaN. The azimuthal alignment of the Si substrate (2 2 4) plane and GaN $(1\,\bar{1}\,0\,5)$ plane was confirmed with X-ray diffraction for samples with thicker layers. In the FESEM images, there are striations clearly visible on the facet walls. These features are less obvious in AFM scans. The striations are probably surface step bunching or reconstructions that cause a variation in surface charging. Finally, we note that the polarity of the matrix material and nanowires is still under investigation. We have used a positive *c*-axis index (Ga-terminated) to allow specific assignment of directions, but the planes and directions could in fact require negative *c*-axis indices (N-terminated) to accurately represent the polarity of the crystals.

The V:III ratio is known to be a critical parameter in the spontaneous formation of GaN nanowires in MBE [7,9,10]. The data in Fig. 1 support a model in which a higher V:III ratio or greater atomic N concentration increases the nucleation density of nanowires. The approximate wire densities for the growth runs represented in Fig. 1 are 2, 2, 37 and 22 wires/μm^2, for (a) through (d), respectively. These data indicate that the N species

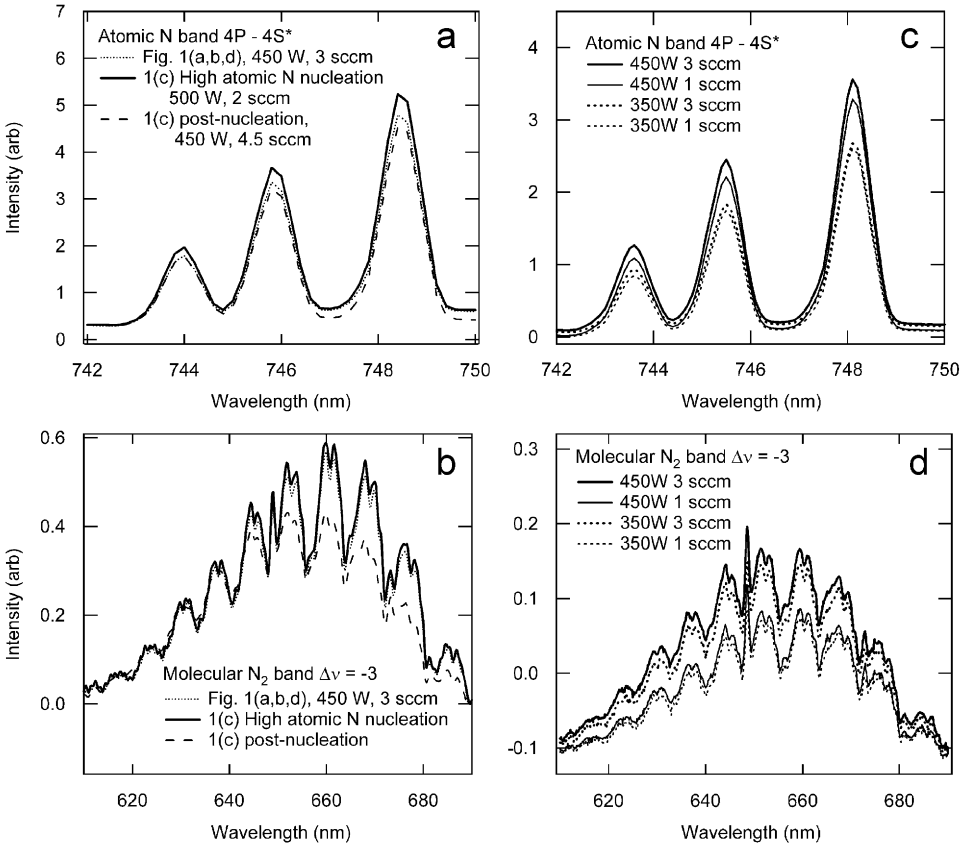

Fig. 4. Optical emission for different N_2 plasma conditions for spectral regions representing (a and c) atomic N lines and (b and d) excited molecular N_2.

composition, in particular the presence of atomic N, has greater influence on the nucleation density than does the Ga flux. Unfortunately, there is a great deal of variability in the N species produced by plasma sources over time and between different source designs. We have monitored the optical emission from the N_2 plasma for our system, and the results for spectral regions representing atomic N lines (a and c) and excited molecular N_2 (b and d) are given in Fig. 4. The graphs in Fig. 4(a) and (b) illustrate spectra from the plasma source when operated under the growth conditions used for the runs represented in Fig. 1. The alteration of the plasma power and gas flow rate that produced higher density wire nucleation (Fig. 1(c)) also increased the intensity of the atomic nitrogen lines. The plasma conditions for the last two-thirds of this run were altered so that the atomic N concentration returned to a typical level, while the excited molecular species concentration was reduced. Given that the hexagonal pit formation begins immediately upon the initiation of growth, it is unlikely that this change had any effect on the morphology. We have seen more dramatic changes in nanowire and matrix morphologies for longer growth runs with plasma conditions represented by the spectra in Fig. 4(c) and (d). The nucleation of nanowires was increased for growth runs with 450 W power, which Fig. 4(c) indicates as producing higher atomic N flux. The total growth rate of nanowires and matrix layers was found to be increased by higher gas flow regardless of RF power, which Fig. 4(d) indicates as producing higher excited molecular N_2 species. (The FESEM images for these growth runs are in Ref. [1].)

Although N species and temperature clearly play a role in nanowire nucleation, we have also observed a strong dependence on the AlN buffer layer thickness, as illustrated in Fig. 5. Fig. 1(a) represents the same growth conditions with a thinner buffer layer of 50 nm. More remarkably, no deposition of either matrix layer or nanowires occurred when growth proceeded with the same substrate heat treatment and GaN nucleation conditions but omitted the Al pre-layer and AlN buffer layer. Instead, a slightly irregular amorphous layer, possibly SiN_x, formed with total thickness of less than 20 nm. Increasing the AlN buffer layer thickness substantially increased the nanowire density and reduced the size of the hexagonal pits. These findings demonstrate that AlN provides an essential template for nanowire nucleation, which was earlier suggested by our study of nanocolumn formation in AlN buffer layers [11]. On the other hand, at least two other groups have reported [1,12,13] that they have found MBE nanowire growth conditions that do not require AlN buffer layers. It is likely that these discrepancies arise from differences in the substrate outgas procedures and growth system hardware (such as manipulator heater environments) that in turn affect SiN_x formation in the early stages of growth.

Further elucidation of the conditions necessary for nanowire formation is given by the data in Fig. 6, which

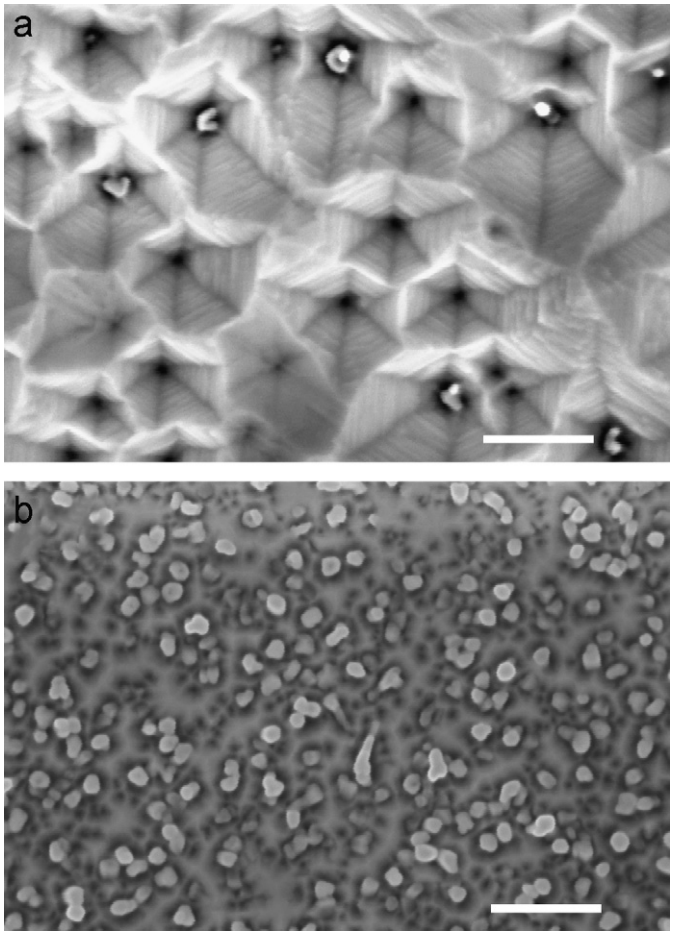

Fig. 5. FESEM images showing that nanowire density increased when the AlN layer thickness was increased. (a) AlN buffer 60 nm, wire density 5 wires/μm^2 and (b) AlN buffer 80–100 nm, 160 wires/μm^2. These layers were otherwise grown with the same conditions as for the specimen illustrated in Fig. 1(a), 2 wires/μm^2. Marker bars indicate 200 nm.

illustrate the morphologies evident in specimens grown (a and b) on Si (1 0 0) substrates, and (c and d) with NH_3 as the sole N source. Nanowires readily form on Si (1 0 0), and X-ray diffraction confirmed that these nanowires have a strong *c*-axis orientation, based on the presence of (0 0 2) and (0 0 4) diffraction peaks in $2\theta-\omega$ scans for both GaN and AlN. The absence of asymmetric diffraction peaks from the nanowires on Si (1 0 0), in contrast to low-intensity peaks from nucleation layers on Si (1 1 1), suggests that the relative azimuthal alignment of the nanowires grown on Si (1 0 0) was more random than for nucleation on Si (1 1 1). The Si (1 0 0) wires also appear more irregular in cross-section in Fig. 6(a) and (b). It thus seems that while the Si substrate provides a template for nanowire growth, there is also a driving force for the formation of *c*-axis wires regardless of the starting orientation of the substrate. The growth with NH_3 produced no nanowires but high hexagonal pit density. Some of these pits contained steep sidewalls similar in form to nanopipe formation reported in MBE GaN films grown with high N flux. This result provides additional support for the role of atomic N in the nucleation of the nanowires.

We also observed that there may be additional variability in plasma source conditions or interaction with other growth parameters that goes beyond simple V:III ratio or buffer layer thickness dependence. The changes observed in the morphology in Figs. 1 and 5 were in some cases disproportionate to the changes in growth parameters. Samples grown near one another in time sequence (Figs. 1(a and b) and 5(a)) were often more like each other than samples grown several weeks later with only slightly different parameters (Figs. 1(c and d) and 5(b)). Greater refinement of in situ monitoring may assist in making firmer ties between growth morphology and growth conditions.

The data contained in this and previous papers [7,8] provide the basis for a model in which nanowires nucleate and propagate through the formation of specific crystal planes that have different sticking coefficients for Ga. In particular, if the *c*-plane at the end of the nanowires has a higher sticking coefficient than the sidewalls of the nanowires or hexagonal pits, the nanowires will propagate along the *c*-direction. The degree of lateral versus longitudinal growth will depend on the surface mobility of the atoms and on the difference in sticking coefficients. The high temperatures and low Ga fluxes required for nanowire growth are consistent with a mechanism that involves long surface diffusion lengths. The morphology will be similar to that produced by catalytic growth because the catalyst plays the role of enhancing the sticking coefficient for reagents at the end of a wire, once nucleated. The stable planes observed in the growth are either nonpolar $\{\bar{1}\,1\,0\,0\}$ planes for the nanowire sidewalls or quasi-nonpolar $\{\bar{1}\,1\,0\,2\}$ planes for the matrix. The stability probably arises from the combination of low polar energy and low dangling bond density. Recent theoretical work [14] indicates that the $\{0\,0\,0\,1\}$ planes have the high growth velocity for GaN under thermal equilibrium, and that minima occur in the $\langle 1\,0\,\bar{1}\,1\rangle$ directions. There are saddle points in the model, however, and the model also predicts high growth velocity in the $\langle 1\,1\,\bar{2}\,0\rangle$ directions as well. Because the $\{1\,1\,\bar{2}\,0\}$ planes are at right angles to the slower-growing $\{\bar{1}\,1\,0\,0\}$ planes, initial growth excursions along the $\langle 1\,1\,\bar{2}\,0\rangle$ directions might terminate through the formation of $\{\bar{1}\,1\,0\,0\}$ sidewalls. The role of atomic N appears to be one of stabilizing the formation of *c*-plane regions on the AlN buffer surface. Once nucleated, the *c*-axis growth mode is highly favored, as demonstrated by the dominance of this mode for both Si (1 0 0) and Si (1 1 1) substrates.

4. Conclusion

Spontaneous formation of *c*-axis GaN nanowires in MBE was analyzed under a number of different growth conditions, including relative flux of N species to Ga, type of N species present, AlN buffer layer thickness, and

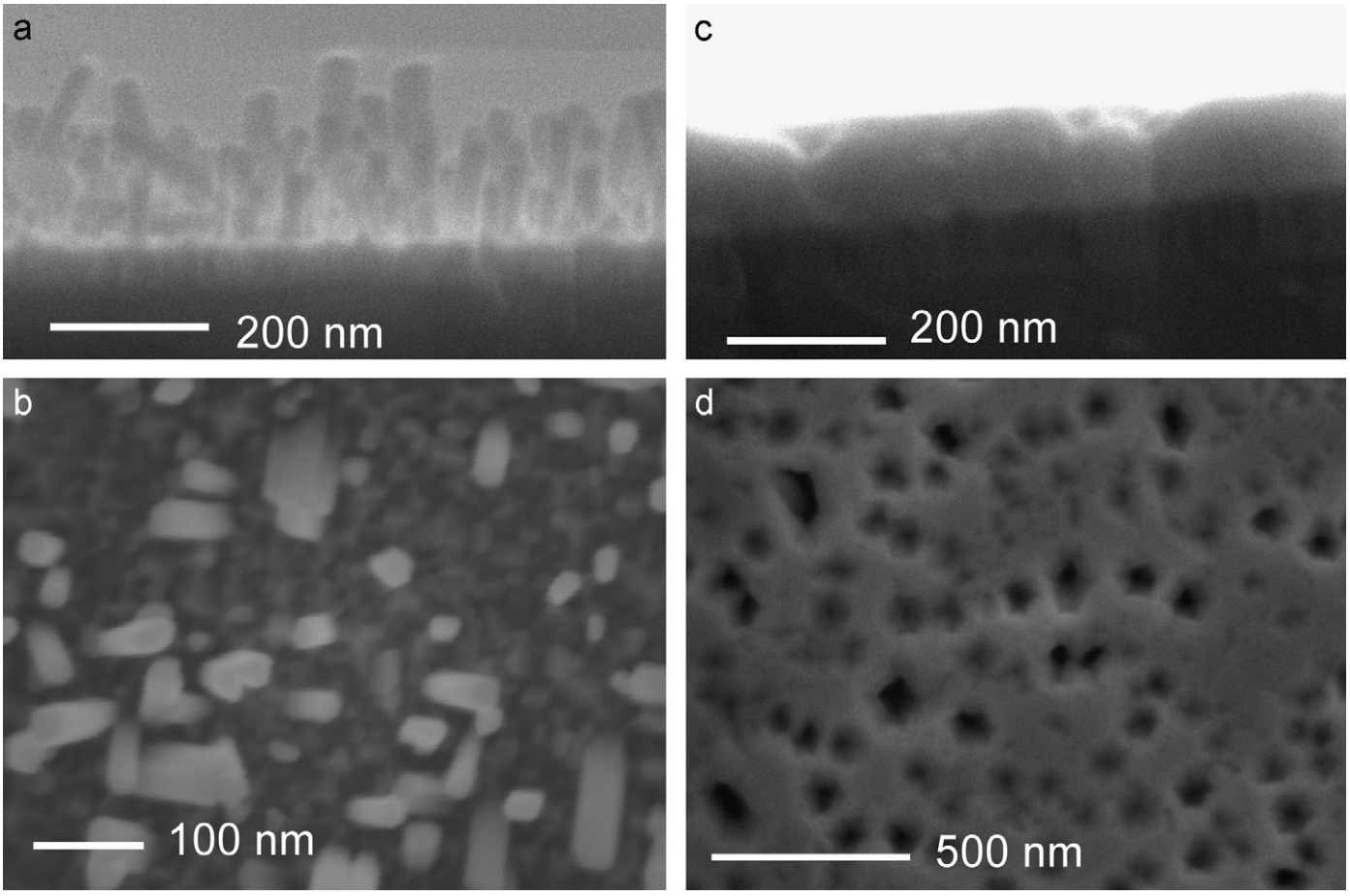

Fig. 6. FESEM images for nanowire nucleation on Si (1 0 0) with plasma N_2: (a) side view and (b) plan view; and on Si (1 1 1) with NH_3 as the only source of nitrogen: (c) side view and (d) plan view.

substrate orientation. Nucleation of nanowires was found to be highly correlated with the formation of hexagonal pits with $\{\bar{1}\,1\,0\,2\}$ facets. The presence of both the AlN buffer layer and atomic N appear to be necessary for the nucleation of nanowires in our growth system. We explain the results in terms of a model in which the sticking coefficient at the polar end of the nanowire is substantially higher than at either the nonpolar sidewalls or the quasi-nonpolar hexagonal pits facets.

References

[1] A. Kikuchi, M. Kawai, M. Tada, K. Kishino, Jpn. J. Appl. Phys. 43 (P. 2) (2004) L1524.
[2] H.-M. Kim, Y.-H. Cho, H. Lee, S.I. Kim, S.R. Ryu, D.Y. Kim, T.W. Kang, K.S. Chung, Nano-Lett. 4 (2004) 1059.
[3] Z. Zhong, F. Qian, D. Wang, C.M. Lieber, Nano-Lett. 3 (2003) 343.
[4] J.C. Johnson, H.-J. Choi, K.P. Knutsen, R.D. Schaller, P. Yang, R.J. Saykally, Nat. Mater. 1 (2002) 106.
[5] J. Ristić, E. Calleja, S. Fernandez-Garrido, A. Trampert, U. Jahn, K.H. Ploog, M. Povoloskyi, A. Di Carlo, Phys. Stat. Sol. A 202 (2005) 367.
[6] E. Stern, G.G. Cheng, E. Cimpoiasu, R. Klie, S. Guthrie, J. Klemic, I. Kretzschmar, E. Steinlauf, D. Turner-Evans, E. Broomfield, J. Hyland, R. Koudelka, T. Boone, M. Young, A. Sanders, R. Munden, T. Lee, D. Routenberg, M.A. Reed, Nanotechnology 16 (2005) 2941.
[7] K.A. Bertness, A. Roshko, N.A. Sanford, J.M. Barker, A.V. Davydov, J. Crystal Growth 287 (2006) 522.
[8] K.A. Bertness, N.A. Sanford, J.M. Barker, J.B. Schlager, A. Roshko, A.V. Davydov, I. Levin, J. Electron. Mater. 35 (2006) 576.
[9] M.A. Sánchez-García, J.L. Pau, F. Naranjo, A. Jimenez, S. Fernandez, J. Ristić, F. Calle, E. Calleja, E. Munoz, Mater. Sci. Eng. B 93 (2002) 189.
[10] M. Yoshizawa, A. Kikuchi, M. Mori, N. Fujita, K. Kishino, Jpn. J. Appl. Phys. 36 (P. 2) (1997) L459.
[11] K.A. Bertness, A. Roshko, N.A. Sanford, J.B. Schlager, M.H. Gray, Phys. Stat. Sol. (c) 2 (2005) 2369.
[12] J. Ristić, M.A. Sánchez-García, E. Calleja, J. Sanchez-Paramo, J.M. Calleja, U. Jahn, K.H. Ploog, Phys. Stat. Sol. A 192 (2002) 60.
[13] J. Ristić, M.A. Sánchez-García, J.M. Ulloa, E. Calleja, J. Sánchez-Paramo, J.M. Calleja, U. Jahn, A. Trampert, K.H. Ploog, Phys. Stat. Sol. B 234 (2002) 717.
[14] D. Du, D.J. Srolovitz, M.E. Coltrin, C.C. Mitchell, Phys. Rev. Lett. 95 (2005) 155503.